Production Evaluation of 255 nm UV LEDs as a Replacement for Mercury Lamps for Wafer Edge Exposure Processes

MERRITT CONNER, Microchip Technology Inc.
PRATIBHA SHARMA and **SAYA HAN,** Violumas Inc.

A 255 nm UV LED array is evaluated as a replacement for a 248.7 nm mercury lamp in a production wafer edge exposure (WEE) system.

WAFER EDGE EXPOSURE (WEE) IS A critical process step in semiconductor manufacturing, used to define clean boundaries and remove unwanted resist near wafer edges [1]. Applications include circular edge trimming, scribe line clearing, and notch region exposure. These steps are essential for ensuring downstream process integrity, particularly during etch and deposition.

Mercury arc lamps have long been the dominant light source for WEE systems due to their strong emission near the 248 nm absorption band of KrF photoresists.

However, despite their widespread use, mercury lamps present several limitations in modern high-throughput manufacturing environments. Over time, mercury lamps experience output degradation due to electrode erosion, material deposition within the arc tube, and solarization of the quartz envelope. These mechanisms reduce optical transmission and lead to intensity drift. As a result, exposure systems require frequent recalibration and periodic lamp replacement to maintain process stability. In addition, mercury lamps operate with high thermal load and constant power consumption, even during idle conditions.

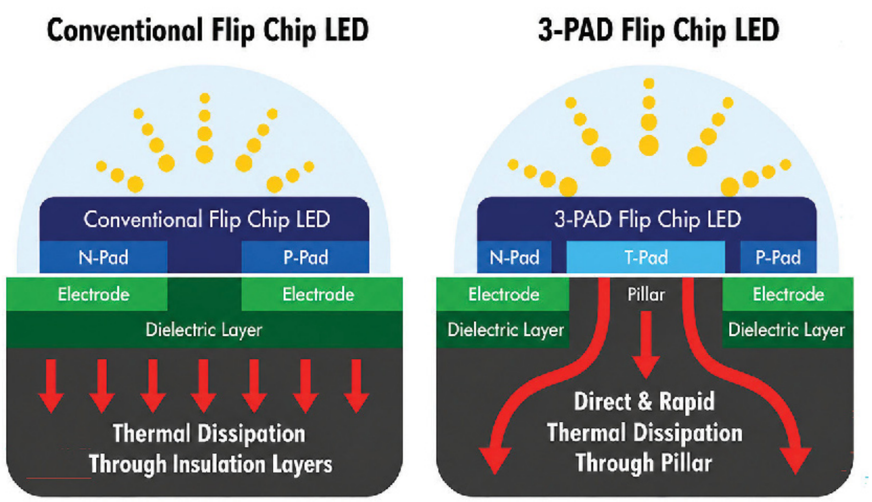

Figure 1. Comparison of the structure of a conventional 2-PAD flip-chip LED with a 3-PAD flip-chip LED with a thermal channel for efficient heat extraction.

The industry's transition away from mercury is increasingly driven by global regulatory frameworks, most notably the *Minamata Convention on Mercury* [2], which mandates the phase-out of mercury-added products in industrial settings to reduce environmental and health risks. Furthermore, modern semiconductor facilities are prioritizing initiatives to meet sustainability goals, including reducing carbon footprint and waste [3].

Ultraviolet light-emitting diodes (UV LEDs) offer a compelling alternative and as a core component of this shift, offer a significant reduction in energy consumption compared to traditional discharge lamps while eliminating the hazardous wastes associated with lamp disposal.

This study evaluates whether a 255 nm UV LED array can replace a mercury lamp in a production WEE system without compromising process performance, while also delivering measurable improvements in operational efficiency.

Commercially available UV LEDs

Over the past decade, UV LED technology has progressed rapidly, enabling practical deployment in commercial systems [4]. Early UV-C LEDs were limited by low output power, short lifetimes, and low wall-plug efficiency, restricting their use primarily to sensing or low-dose applications. However, advances in AlGaN epitaxial growth, chip architecture, and packaging have significantly improved device performance in the 240–280 nm wavelength range.

Modern UVC LEDs are based on aluminum gallium nitride (AlGaN) semiconductor heterostructures grown on sapphire, silicon carbide, or AlN substrates [5]. Improvements in crystal quality and reduction in defects have enabled higher internal quantum efficiency and improved current injection efficiency. At the same time, innovations in optical extraction structures, including patterned substrates and reflective electrode designs, have increased usable optical output.

As a result, commercially available UV-C LEDs now deliver optical power levels reaching greater than 100 milliwatts per chip in the 255-275 nm range, with wall-plug efficiencies approaching 5–10% depending on wavelength and drive conditions. When assembled into multichip arrays, these devices can produce irradiance levels suitable for demanding industrial applications, including semiconductor processing.

Packaging and thermal management have also evolved significantly. High-power UV-C LEDs are typically integrated into ceramic or metal-core packages that provide improved thermal conduction and optical stability under high current densities. Advanced packaging techniques such as the 3-PAD technology (**FIGURE 1**) allow for efficient heat extraction without an increase in thermal budget [6].

High density modules are available in various form factors, incorporate heatsinks along with fused silica lenses, and have optimized circuit design to maintain stable output over extended operating periods (**FIGURE 2**).

Equally important for semiconductor manufacturing is the inherent spectral stability of LED sources. Unlike mercury discharge lamps, which generate broadband emission with multiple spectral lines and can experience spectral shifts as electrodes age, UV LEDs emit within a narrow spectral band typically 10–15 nm wide. This narrowband emission improves spectral predictability and reduces out-of-band radiation that may contribute to unwanted photochemical activation.

Lifetime performance has also improved substantially. While early UVC LEDs exhibited rapid output degradation, current devices can achieve operational lifetimes reaching or exceeding 10,000 hours under properly managed thermal conditions. This represents a significant improvement over mercury lamps, which typically require replacement after a few thousand hours of operation and may exhibit significant intensity drift during their lifetime.

These technological advances have enabled UVC LED systems to transition from laboratory demonstration devices to practical industrial light sources. Applications now include water and surface disinfection, curing, spectroscopy, gas sensing, and increasingly, semiconductor manufacturing processes such as wafer inspection, resist exposure, and wafer edge exposure.

In the context of wafer edge exposure systems, these improvements are particularly significant. The combination of higher optical output, narrow spectral bandwidth, improved reliability, and modular scalability allows LED arrays to deliver the irradiance levels required for production lithography [7] support processes while maintaining the operational advantages inherent to solid-state light sources.

The 255 nm LEDs evaluated in this study represent a new generation of high-power UVC emitters - with integrated advanced thermal packaging (3-PAD) and providing a wavelength closely aligned with the absorption band of KrF photoresists. As demonstrated in the following sections, these devices are now capable of meeting the performance requirements of production wafer edge exposure systems while offering improvements in operational stability and system efficiency.

Spectral considerations

The effectiveness of a light source in WEE applications is strongly influenced by its spectral alignment with the photoresist absorption band.

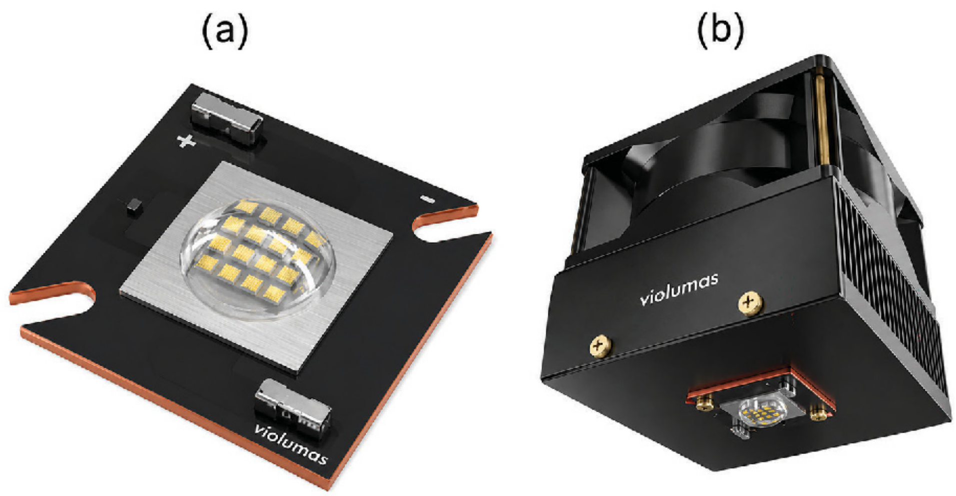

Figure 2. (a) High-density UV LED module (b) with a thermal solution.

KrF chemically amplified resists exhibit peak absorption near 248 nm, with decreasing sensitivity at longer wavelengths.

The mercury lamp used in this study emits a broadband spectrum with a strong line at 248.7 nm, closely aligned with the resist's peak photosensitivity. However, it also produces out-of-band radiation that can contribute to unwanted exposure effects, particularly at higher doses.

The 255 nm LED operates slightly offset from the peak absorption but remains well within the effective reaction band of the resist. In contrast, the 265 nm LED lies further from the absorption peak, resulting in similar though reduced photochemical efficiency. The 265nm LED was included in this study due to the higher radiant flux, lower costs and wider commercial availability.

These spectral differences are reflected in the measured dose response behavior, providing a useful framework for evaluating source performance (**FIGURE 3**).

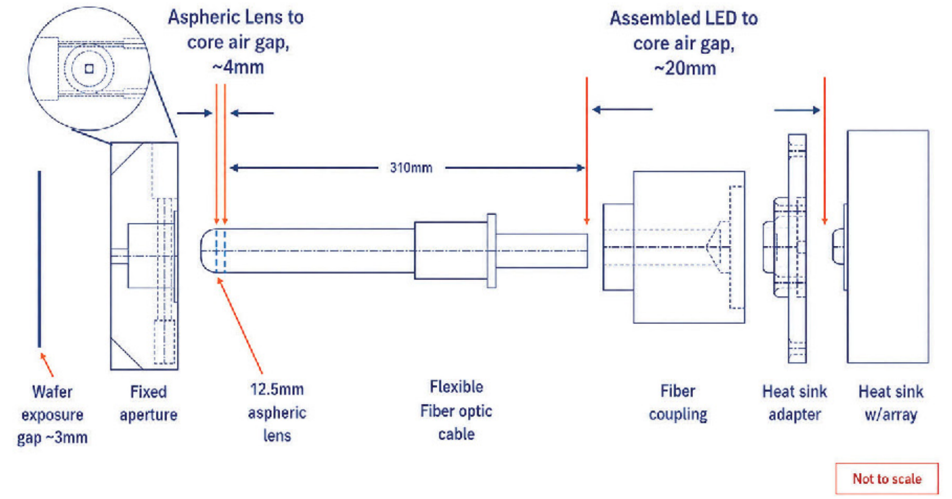

Figure 4. Simplified sketch of the optical train.

Experimental methodology

All experiments were conducted on a TEL ACT8 coat/develop platform equipped with an integrated wafer edge exposure module. The study was designed as a controlled, head-to-head comparison of exposure sources under production-representative conditions.

Process Conditions: The resist stack consisted of an 8500 Å (0.85 µm) thick layer of JSR M91Y KrF chemically amplified resist coated on 6-inch bare silicon wafers. Bottom anti-reflective coating (BARC) was intentionally omitted to avoid optical damping effects and to ensure that observed resist behavior reflected intrinsic photochemical response.

A standard 90-second development process was used across all conditions. Holding development parameters constant ensured that differences in resist clearing were attributable solely to exposure conditions. **FIGURE 4** shows the simplified sketch of the optical train.

Exposure Sources: Three light sources were evaluated:

- 248.7 nm OEM recommended mercury arc lamp (baseline)
- 255 nm High Density 3-PAD UV-C LED array (Violumas, Inc.)
- 265 nm High Density 3-PAD UV-C LED array (Violumas, Inc.)

Each source was calibrated independently to ensure accurate irradiance measurement at the wafer plane.

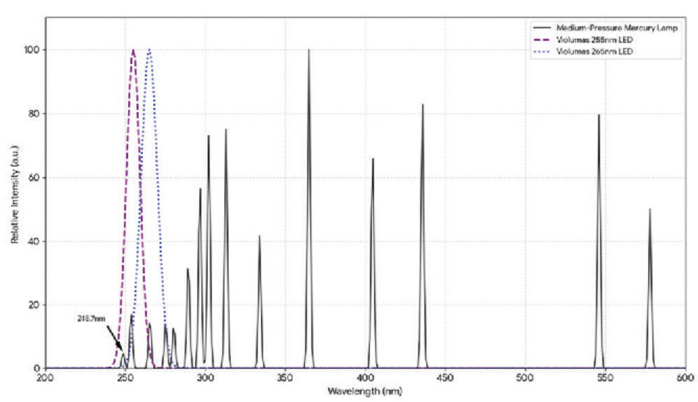

Figure 3. Spectral profile of mercury, 265nm and 255nm LEDs.

Dose delivery was controlled through exposure time and scan speed, enabling consistent energy density comparisons.

All sources were operated under stable conditions to eliminate transient effects.

Results

Dose-to-Clear Performance: The 255 nm LED demonstrated consistent and repeatable dose-to-clear behavior across the evaluated range. The resist exhibited a clear transition from unexposed to fully cleared regions, indicating a strong and stable photochemical activation. The 265 nm LED followed a similar trend, but with degraded response consistency at higher power levels. By comparison, the Hg lamp produced measurable resist reaction only at significantly higher energy settings and with the added burden of unnecessary spectral output (FIGURE 5).

Compared to the mercury lamp, the 255 nm UV LED array achieved:

- Equivalent or improved response was observed at low doses
- No loss in clearing capability was detected within standard process windows
- Dose response remained gradual and controllable, enabling precise threshold definition

The 265 nm LED required higher doses to achieve similar clearing,

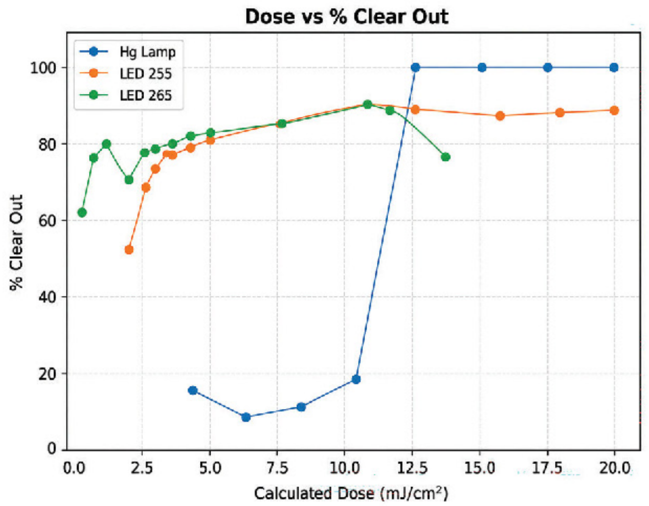

Figure 5. Percent clear out to calculated dose for each light source.

consistent with reduced absorption efficiency of the longer wavelength.

These results confirm that the 255 nm LED provides sufficient energy coupling to the resist for effective edge clearing without introducing process penalties.

Fringe angle and edge profile: Fringe angle, referred to here as edge slope extension, was evaluated as a function of delivered dose to assess how each light source influenced edge sharpness and profile stability. In practical wafer edge exposure terms, a sharper angle is generally preferred because it reflects a more abrupt edge transition, tighter confinement of the exposure boundary, and less unintended lateral resist activation.

The edge-profile images (**FIGURES 6** and **7**) provide the first view of this behavior. In the visual comparisons, the mercury source shows a broader and more rounded transition region as dose increases, indicating that the exposed edge becomes less sharply defined under higher-dose conditions. By contrast, the 255 nm LED maintains a steeper and more controlled edge shape across the evaluated range. These images suggest that the LED source is less prone to profile degradation as dose increases.

FIGURE 8 confirms this trend quantitatively. The Hg source exhibited a measurable reduction in fringe angle at elevated dose levels, consistent with progressive edge broadening under over-dose conditions. The 255 nm LED, in contrast, maintained fringe angle stability and in some dose regions showed improved edge behavior as dose increased. The 265 nm LED showed intermediate performance but did not match the edge stability observed with the 255 nm source.

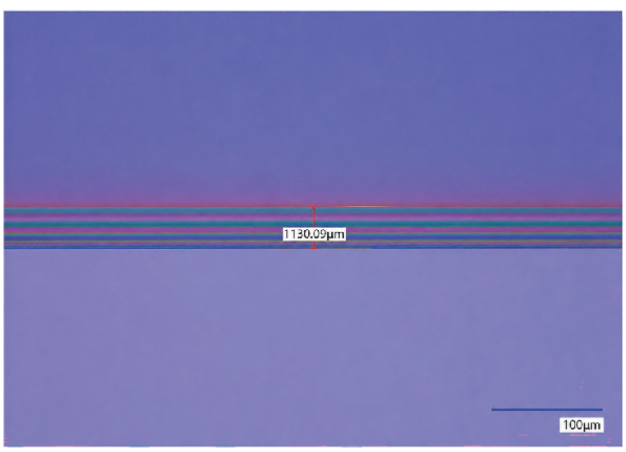

Figure 6. Top-down optical micrograph of the wafer edge exposure region, showing interference fringe structure at the resist boundary. The measured fringe spacing corresponds to an approximate slope of the exposure transition.

This behavior is consistent with the narrower spectral output of the LED source. By concentrating delivered energy more closely within the effective absorption region of the KrF resist, the 255 nm LED reduces out-of-band excitation and helps limit lateral energy spread within the resist film. The result is a steeper and more stable edge profile over a wider usable dose range.

From a manufacturing perspective, this is an important result. A source that preserves edge sharpness as dose varies provides greater process latitude and improved robustness against over-exposure. In this study, the 255 nm LED delivered that advantage relative to the broadband Hg lamp, supporting its use as a more stable and production-friendly light source for wafer edge exposure.

Operational performance

In addition to resist response, operational and electrical characteristics were evaluated under comparable 200 VAC supply conditions to assess production impact beyond lithographic performance.

UV LED Module

1. Power consumption: 36 W (idle), 70 W (active)
2. Temperature: 24 °C (idle), 28 °C after 60 seconds as measured on the heatsink
3. Instant-on operation with no warm-up
4. Stable output with no flicker
5. Minimal thermal rise

Mercury Lamp

- Power consumption: 500 W (constant)
- Temperature: 76 °C (steady state) recorded on the exterior of the light source enclosure, which is mounted inside the tool above the process area.
- Requires warm-up and stabilization
- Continuous high thermal load

The UV LED system demonstrated significantly lower power consumption and reduced thermal impact.

Discussion

Process Capability: The 255 nm LED achieved equivalent or improved resist clearing compared to the mercury lamp. Its stable fringe angle behavior at higher doses indicates improved edge robustness and reduced sensitivity to over-exposure.

Importantly, no reduction in process window was observed, confirming that the LED can be implemented without compromising manufacturing performance.

Tool Stability: Unlike mercury lamps, LED sources do not rely on plasma discharge and therefore do not exhibit flicker or arc instability. Their spectral output remains consistent over time, reducing intensity drift and improving dose repeatability.

This stability reduces the need for frequent recalibration and enhances overall process control.

Operational Efficiency: The LED system offers several advantages:

- Instant-on operation eliminates warm-up delays
- Lower power consumption reduces energy costs
- Reduced thermal load simplifies thermal management
- Longer lifetime eliminates frequent replacement cycles

These benefits translate directly into improved tool uptime and reduced maintenance burden.

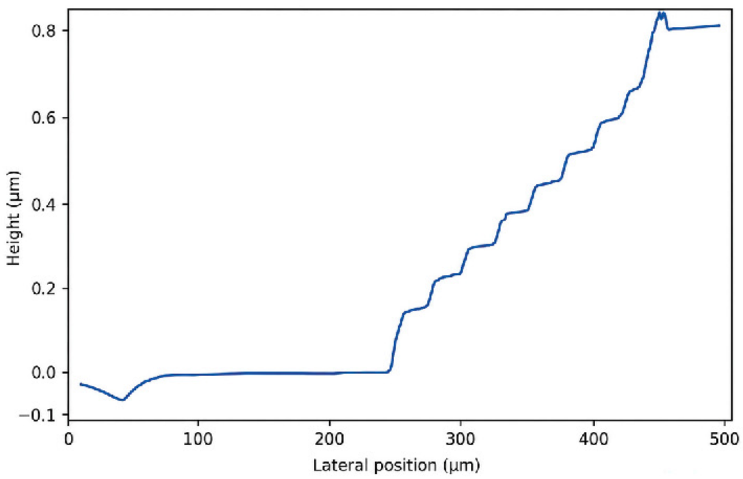

Figure 7. Reconstructed profilometer trace of the wafer edge region, generated from legacy screen-captured data for clarity. The measured profile shows a gradual slope consistent with fringe-derived edge transition behavior.

edge exposure systems.

The LED source delivers equivalent or improved resist activation, enhanced edge profile stability, and greater tolerance to dose variation. In addition, it offers significant advantages in power efficiency, thermal management, and operational stability.

The transition from mercury-based illumination to solid-state UV LEDs represents a practical and scalable upgrade path for

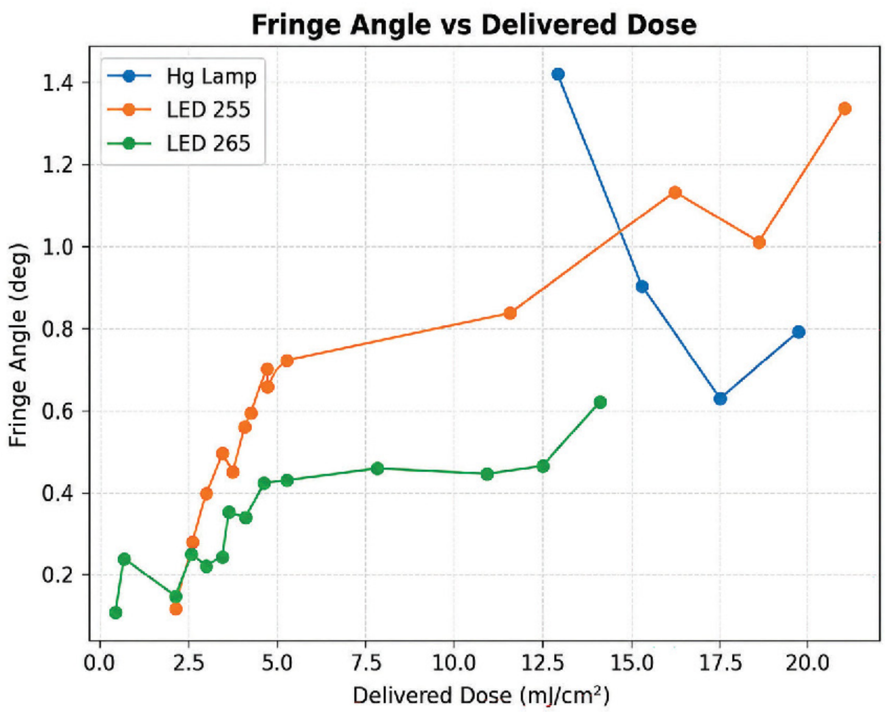

Figure 8. Fringe angle vs delivered dose for the three light sources.

Cost of ownership and ROI operating cost impacts

From a manufacturing perspective, the transition to LED-based WEE systems provides clear economic benefits:

- Elimination of lamp replacement costs
- Reduced downtime for maintenance
- Lower energy consumption
- Simplified system architecture

Collectively, these factors contribute to a lower total cost of ownership and improved operational efficiency. After the initial capital expense of conversion, an approximate annual cost saving of over 90% can be gained from the transition to LED-based light sources (**FIGURE 9**).

Conclusion

This study demonstrates that 255 nm UV LEDs can serve as a viable replacement for mercury arc lamps in DUV wafer

Continued on page 28

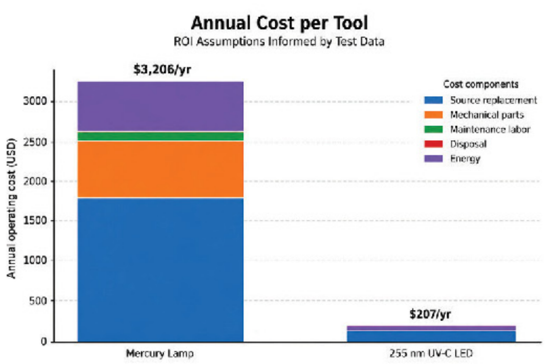

Figure 9. Cost comparison with LED and incumbent technology

r CMP polish time to maintain dimensional control.

For complex nonlinear processes like Reactive Ion Etch (RIE), Reinforcement Learning (RL) offers a powerful solution. Rather than relying on physical models, an RL controller learns through interaction with the environment, guided by rewards such as yield and C_{pk}. This enables optimization of bias power and gas ratios to adjust or re-tune for chamber wall polymerization without manual tuning.

Practical applications and roadmap

The efficacy of this framework is most evident when transitioning from theoretical concept to an active fab environment. In a recent pilot targeting the early-stage ramp of an advanced node (e.g., 5nm/7nm) at one of the leading foundries, process engineers utilized this APC framework to address critical patterning bottlenecks, including pitch-walk issues in hybrid metrology. By allowing real-time chamber stability and C_{pk} performance to dictate sampling plans, this implementation drove a 38% reduction in physical CD-SEM usage (usually a bottleneck in modern-day metrology) and improved overall cycle time by 22%. Ultimately, this approach enabled manufacturers to recapture hundreds of hours of tool capacity without compromising excursion sensitivity or product yield. Continuous VM and statistical capability estimates have reduced false lot holds by about 20%, minimizing unnecessary engineering troubleshooting and maintaining production capacity.

These concepts converge in critical modules. In lithography and etch, ML models correlate scanner dosage to CD outcomes – allowing downstream etch equipment to proactively compensate for upstream variations and reducing issues like line-edge roughness (LER). In CMP and Deposition, ML models analyze torque and vibration to detect emerging scratches triggering immediate corrective action.

C_{pk}-based adaptive sampling, machine learning-driven virtual metrology, and closed-loop control represent a structural shift in yield ramp strategy. Instead of relying on static plans, manufacturers deploy responsive, risk-averse systems that allocate metrology capacity based on statistical evidence. For foundries and IDMs operating at advanced nodes, this approach accelerates ramp, protects reliability, and preserves margin.

About the Author

Anshul Karnik is a Senior Product Quality Manager at a global consumer electronics leader, where he oversees NPI quality engineering for flagship mobile hardware programs manufactured at advanced semiconductor nodes and deployed at global production scale. With more than a decade in semiconductor manufacturing, he has led technology development and quality initiatives spanning NPI, yield ramp, and high-volume production at leading foundries, advancing data-driven test strategies, AI/ML-enabled predictive analytics, and statistically grounded process control methodologies. His current responsibilities include integrating adaptive sampling, virtual metrology, and closed-loop optimization frameworks to accelerate yield ramp, reduce metrology bottlenecks, and strengthen process stability in advanced-node manufacturing environments supporting high-volume consumer device ecosystems.

 Continued from page 21

semiconductor manufacturing, enabling improved process control while reducing operational complexity. All results in this study were achieved using commercially available UVC LED devices. With ongoing improvements in optical output, wall-plug efficiency, and lifetime, the relative benefits of UVC LED-based systems are expected to become increasingly pronounced.

Acknowledgement

The authors gratefully acknowledge Microchip Technology Inc. for its support in conducting the test work and collecting the data presented in this paper.

REFERENCES

1. Mack, C. A. (2007). Fundamental Principles of Optical Lithography: The Science of Microfabrication. John Wiley & Sons.
2. Website: https://minamataconvention.org/en/about/convention-text
3. Yin Y, Yang Y. Sustainable Transition of the Global Semiconductor Industry: Challenges, Strategies, and Future Directions. *Sustainability.* 2025; 17(7):3160. https://doi.org/10.3390/su17073160
4. Bhattarai, T., Ebong, A., & Raja, M. Y. A. (2024). A Review of Light-Emitting Diodes and Ultraviolet Light-Emitting Diodes and Their applications. *Photonics, 11*(6), 491. https://doi.org/10.3390/photonics11060491
5. Yuxuan Chen, Jianwei Ben, Fujun Xu, Jinchai Li, Yang Chen, Xiaojuan Sun, Dabing Li, Review on the Progress of AlGaN-based Ultraviolet Light-Emitting Diodes, Fundamental Research, Volume 1, Issue 6,2021,717, https://doi.org/10.1016/j.fmre.2021.11.005.
6. Website: https://violumas.com/our-technology/
7. Hölz K, Lietard J, Somoza MM. High-Power 365 nm UV LED Mercury Arc Lamp Replacement for Photochemistry and Chemical Photolithography. ACS Sustain Chem Eng. 2017 Jan 3;5(1):828-834. doi: 10.1021/acssuschemeng.6b02175.